

Non-Invasive Measurement of Intracranial Pressure Through Application of Venous Ophthalmodynamometry

Lachlan Lo, Da Zhao, Lauren Ayton, David Grayden, *Senior Member, IEEE*, Bang Bui, Andrew Morokoff and Sam John, *Member, IEEE*

Abstract — Non-invasive intracranial pressure (ICP) monitoring is possible using venous ophthalmodynamometry to observe a pulsation in retinal blood vessels when intraocular pressure (IOP) exceeds ICP. Here, we identify features in the eye – optic disc and retinal blood vessel locations – and identify pulsation in large retinal blood vessels. The relationship between force and the magnitude of pulsation is used to estimate ICP when force is applied to the eye to gradually increase IOP over time. This approach yields 77% accuracy in automatically observing vessel pulsation.

Clinical Relevance — Non-invasive ICP monitoring is desirable to improve patient outcome by reducing potential trauma and complications associated with invasive assessment with intracranial sensors or lumbar puncture.

I. INTRODUCTION

In traumatic brain injury, it is necessary for first responders and doctors to make rapid and accurate measurements of intracranial pressure (ICP). Elevated ICP is an important indicator of pathological conditions such as swelling or bleeding of the brain [1] and, without rapid treatment, these conditions can quickly lead to hyperemia and cerebral oedema associated neuronal damage [2] [3].

The current gold standard for ICP measurement is a ventriculostomy catheter [4], where a pressure transducer is connected directly to the fluid-filled cavities of the brain. However, this is a highly invasive procedure that can lead to complications such as infection or hemorrhage. Additionally, this surgical procedure can only be done in a hospital by a trained surgeon, limiting the accessibility and availability of ICP monitoring.

Drugs exist to treat elevated ICP within 1-5 minutes [4] but cannot be administered without an ICP measurement. As such, remote patients with head injuries must be transported to hospital, with the delayed treatment increasing the risk that they may develop secondary ailments. Therefore, there is a need for a non-invasive, quick method of estimating ICP in order to reduce the risk and time taken to get accurate ICP values.

*Research supported by Hirshom foundation grant (CI Bui) and a University of Melbourne Seed Grant (CI Ayton). L. Lo is with the Department of Biomedical Engineering at the University of Melbourne, Melbourne Australia (e-mail: lachlan.aj.lo@gmail.com) D. Zhao is with the Department of Optometry and Vision Sciences at the University of Melbourne, Melbourne Australia (e-mail: da.zhao@unimelb.edu.au) L. Ayton is with the Departments of Optometry and Vision Sciences, and Surgery (Ophthalmology) at the University of Melbourne, Melbourne Australia (e-mail: layton@unimelb.edu.au)

An avenue for taking non-invasive ICP measurements is using venous ophthalmodynamometry (vODM). In the eye, the optic nerve is surrounded by a sheath of cerebrospinal fluid that has an analogous pressure to ICP. Increasing the intraocular pressure (IOP) to be greater than ICP will cause the veins to deflate due to the resulting pressure difference between the intraocular and retro-laminar optic nerve compartments [5]. When the heart beats, the increase in blood pressure throughout the circulatory system will cause the blood vessels to reinflate briefly. Therefore, at the moment IOP exceeds ICP, there will be a noticeable pulsation in the blood vessels in the eye and, in particular, the veins at a pulsation frequency equal to heart rate. If IOP is gradually elevated over time and the blood vessels observed, then when the vessels start pulsing, the IOP and ICP would be equal. This provides a potential method whereby ICP can be measured via the eye in a non-invasive manner.

The principle of vODM has been examined in both animals [6] and humans [7]. The relationship between ICP and retinal vessel pressures has been shown in studies by Rios-Montenegro et al. [6], where owl monkeys had ICP manually elevated while orbital venous pressure was recorded. It was shown that elevated ICP elicited a noticeable change in orbital venous pressure. The relationship between the ICP and resultant IOP was shown to be linearly correlated.

In a human trial [7], a hand-held device was used to mechanically increase IOP while a hand-held ophthalmoscope detected the pressure in the eye. This was performed on patients with a ventriculostomy catheter already implanted, so ICP values could be known precisely. This study showed that by manually observing vessel collapse, IOP could be correlated to an accurate ICP value with an r value of 0.85. This indicates that ICP detection through vODM is possible. However, manual observation is more prone to error, thus an accurate automated approach to detect changes in pulsatility would be very useful.

In the current study, we created an automated detection method for ICP detection through vODM. Here we automatically detect the optic disc and segment the blood vessels of interest to detect vessel pulsations.

D. Grayden is with the Department of Biomedical Engineering at the University of Melbourne, Melbourne Australia (email: grayden@unimelb.edu.au) B. Bui is with the Department of Optometry And Vision Sciences at the University of Melbourne, Melbourne Australia (e-mail: bvb@unimelb.edu.au) A. Morokoff is with the Department of Surgery at the University of Melbourne, Melbourne Australia (e-mail: morokoff@unimelb.edu.au) S. E John (Corresponding Author) is with the Department of Biomedical Engineering at the University of Melbourne, Melbourne Australia (phone: +61 3 834 49437 ; e-mail: sam.john@unimelb.edu.au)

II. MATERIALS

All animal studies were approved by the Florey Animal Ethics Committee, ethics application 19-070-UM and carefully followed the Australian National Health and Medical Research Council statement on the use of animals in scientific research. The data included a series of videos of retinæ of anesthetized (ketamine:xylazine) adult male and female Long Evans rats (N=9 rats). The inner eyes of these rats were recorded at varying values of IOP for established values of ICP.

The recordings were made with an ophthalmoscope centered on the optic disc of the rat. A 30G cannula was inserted into the eye and a 23G dual-lumen cannula (30G inside) into the lateral ventricle of the brain of each rat to record pressures therein. In each rat, ICP was kept constant and IOP was increased by elevating a saline reservoir to calibrated heights in steps of 10 mmHg with a 10 second color video (30 fps, Micron III, Phoenix, Pleasanton, CA) recorded at each IOP level. These videos were then assembled into one continuous video post-experiment for image analysis. Heart rate in each video was approximated using fluctuations in blood pressure of the rats and was generally around 240 BPM (~4 Hz), as expected during anaesthetization [8].

III. METHOD

Predicting ICP through vODM involves detecting the pressure at which pulsation begins in retinal blood vessels as IOP is elevated. This was approached in two steps: detection of the major blood vessels in the eye and identification of pulsation in these vessels. The coding suite used for this approach was MATLAB ver. 2019a.

A. Detection of vessels

Limiting the information analyzed to the major blood vessels in the fundus helped to improve accuracy by removing potential background noise from non-vessel regions. To do this, specific ‘windows’ were defined over the regions of interest in the videos. Establishing these windows involves identifying the optic disc as the origin of the inner retinal blood vessels, extracting the locations of major vessels in the eye, and reducing these vessel locations to short vessel segments at the optic nerve head. This is done using the first frame of an input rat fundus video as a reference template for the remaining frames in the video sequence.

Detection of the optic disc is performed using a previously established method [9]. This involves identifying the optic disc as a circular region that appears brightly against the background of the rest of the eye. The center of the disc is then defined where there is a sharp intensity change in all directions. This brighter contrast allows for vessel pulsation to be more easily observed.

Identification of blood vessels in the eye is achieved primarily using an existing vessel segmentation method [10]. First, the image is corrected for inhomogeneous brightness to improve segmentation accuracy. This is done by using a mean intensity filter to identify brightness throughout the eye as per a previously described technique [11]. Segmentation is then performed with a series of filter kernels designed under the

assumption that blood vessels can be modelled as Gaussian bodies, with greatest intensity at the center of the vessel and a rapid reduction in intensity going outwards. This is constructed with the following equation and conditions:

$$K(u, v) = -\exp\left(-\frac{u^2}{2\sigma^2}\right) \forall \{u, v\} \in N, \quad (1)$$
$$N = \{(u, v) \mid |u| \leq 3\sigma, |v| \leq L/2\}$$

For filter kernel K , kernel column and row u and v , respectively, standard deviation $\sigma = 5$, kernel length $L = 31$, and effective kernel size N . Convoluting this kernel across the eye image gives greater values when applied over vessels. A set of 12 kernels is generated to act between angles 0° and 165° in increments of 15° . These kernels are applied in a novel technique wherein 12 regions, also in 15° increments, are established rotationally around the optic disc and a filter kernel oriented with the angle of each region is applied throughout. This highlights the blood vessels coming directly from the optic disc, ignoring transverse vessels and other structures like the optic disc. The response of the filter kernels is normalized and binarized to make a mask containing only the vessel locations.

Finally, in a circle around the center of the optic disc, the intensity of blood vessels is measured while frame information not included in the segmentation is colored white. The locations of the five widest vessels – as identified by peaks in intensity along this circle – are used to reduce the vessel mask down to small sections. This vessel mask, shown in Figure 1, is used to measure blood vessel pulsation.

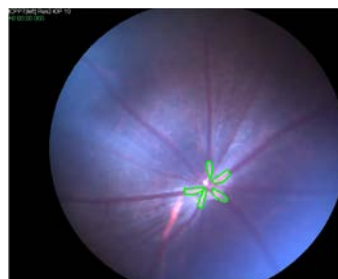


Figure 1. Single frame of a video of a rat fundus showing blood vessels with automatically generated mask overlaid on top (green)

B. Detection of pulsation

Brightness is measured within the established regions of interest. Once IOP exceeds ICP, the retinal vessels pulsate in time with the heart, presenting as a rhythmic increasing and dimming of brightness. Brightness is measured for every frame and a 60-point Fast Fourier transform was applied to the data. Under ketamine and xylazine anesthesia, rats have a heart rate of 200-250 BPM. Therefore, peaks at approximately 4 Hz in the Fourier spectrum are taken to indicate the presence and magnitude of the pulsatility. If this peak is detected in 66% of transforms over 2 seconds, pulsation is considered to be detected in the eye. Hence if pulsation is detected in the eye, the ICP is estimated to be the current value of IOP.

IV.

Pulsation was correctly detected in 77% of the nine fundus videos. This was assessed by comparing vessel pulsatility (if detected at all) to the expected pressure at which pulsation should be present in the fundus video – when IOP exceeds ICP. The variation in latency of this detection was $\pm 4.4s$, from the time when the IOP step increased above ICP. One event was detected before the expected IOP step occurred.

Specificity and sensitivity were also measured. As IOP changes were abrupt (10 mmHg steps), it was possible to characterize a time window video where vessel pulsation should not be occurring as IOP was low ("i" in Figure 2, corresponding to 10 mmHg IOP). Similarly, there was a time window in the video where IOP exceeded ICP (see "ii" and "iii" in Figure 2, corresponding to 20 and 30 mmHg IOP, respectively) and pulsation should be prominent. At low IOP, a small number of frequency peaks at around 4 Hz were detected but these were infrequent. With higher IOP levels, peaks at 4 Hz could be readily detected (see "iii" in Figure 2).

Specificity was measured by counting the number of time points expressing a heart rate peak at low IOP (10 mmHg) which was found to be 93% on average with standard deviation 6.8%. Sensitivity was measured by counting the number of time points without a heart rate peak at high IOP (30 mmHg) and was found to be 38% on average with standard deviation 30%. These results are shown in Table 1.

TABLE I. PULSATION DETECTION RESULTS

Video	ICP (mm Hg)	Correctly identified non-pulsing frames (%)	Correctly identified pulsing frames (%)	Error in pulsation detection
1	16.9 \pm 0.2	100%	100%	+0s
2	15.9 \pm 0.6	96%	4%	Did not detect
3	19.8 \pm 0.2	85%	25%	-2.4s
4	25.2 \pm 1.0	100%	8%	Did not detect
5	14.0 \pm 0.2	83%	33%	+4.4s
6	20.0 \pm 0.6	100%	26%	+2.0s
7	17.3 \pm 0.9	89%	48%	+4.3s
8	20.9 \pm 0.2	96%	32%	+2.6s
9	21.9 \pm 1.4	88%	67%	+0s
Average		93%	38%	\pm 4.4s

By comparing Figures 2B and 2C, it can be seen that pulsation occurred consistently after IOP was increased relative to ICP, similar to previous reports [6]. Further testing is required to assess the specific relationship between the magnitude of pulsatility, IOP, and ICP.

It was additionally found that, when applying the novel blood vessel segmentation process, more artefacts were introduced at the edge of the mask. However, close to the optic disc – the only relevant section of the mask for the program – there was an average reduction of 4144-pixel error with 2800 standard deviation. This equates to an approximately 15 times fewer incorrectly identified pixels

based on the dimensions of the masks. Vessel masks generated by existing methods [10] and novel methods are presented side by side in Figure 3A and 3B. The presence of the optic disc was reduced in particular in all segmentation masks.

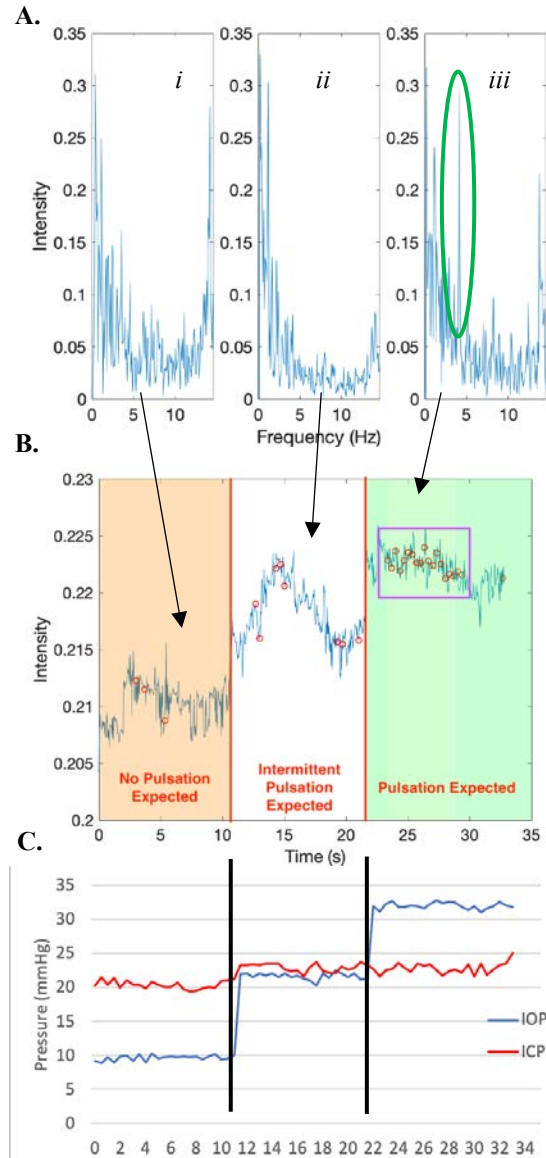


Figure 2. Results of the pulsation detection program. A) Fourier transforms of average light intensity at different times of video 9. It is noted that in plot *iii* the strength of the signal at 4 Hz is strongest (green). B) Results from pulsation detection program for video 9 showing average light intensity through automatically established windows (blue), time points where a heart rate frequency peak was detected in the Fourier transform (red), and where pulsation was detected (purple). Also shown with highlighted regions are where IOP is lower than ICP and no pulsation is expected (orange) and where IOP is greater than ICP and pulsation is expected (green). Central region is where IOP and ICP are too close to see consistent pulsation. Arrows (black) show how Fourier transforms in A. correspond to different regions. C) IOP (blue) and ICP (red) throughout the video 9 with defined points where region changes (black).

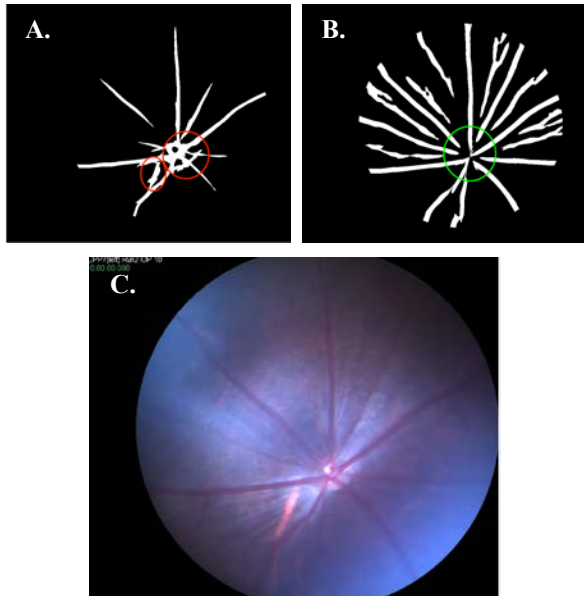


Figure 3. Masks generated by segmentation of blood vessels. A) Mask generated using a method from existing literature with non-vessel structures included (red). B) Mask generated using novel method, notably with optic disk not present (green). C) The original frame of the video showing how vessels are represented in the masks.

V. DISCUSSION

Our results show that pulsation in vessels can be detected via an automatic system in rats. Based on the principles of venous ophthalmodynamometry, the advent of this pulsation can be used to relate pressure in the eye to pressure in the head as a means of non-invasive ICP monitoring. In this study we were able to segment all blood vessels of interest and detect the optic disc, while controlling for extraneous factors like eye movement are controlled for. A detection rate of 77% indicates that vessel pulsation as a result of elevated IOP is a metric that can be detected automatically. These results still lack sufficient accuracy for medical application. In particular, the sensitivity value of $38\% \pm 30\%$ is low. The low sensitivity was likely a result of the experimental set up in a small animal model. Future work should consider using a large animal model with a device that manipulates the IOP externally as well as automatic adjustment for external factors such as lighting which could possibly improve pulsation detection.

Improvements can be made to the method to greatly increase accuracy. The heart rate used to define the frequency of interest was an approximation; changes in heart rate during recordings were not considered in the current approach. In real-world applications of this technique, heart rate could be readily measured and the true rate used to accurately define the frequency of interest. For example, by incorporating ECG methods into future experiments, time-synchronized heart rate data could also be used by the program to determine the expected frequency and times of pulsation. Implementing this would, however, increase the complexity of the device.

Further testing with more subjects, both animal and human, will allow us to determine the specific relationship between

IOP, ICP, and the magnitude of pulsation observed, including the threshold of IOP relative to ICP required to induce pulsation.

Finally, improvement of vessel segmentation was achieved compared to existing techniques. Features like the optic disc were excluded from the final mask. Although the improvement varied in effectiveness, it always reduced the number of artefacts near the optic disc. This technique was relevant only to the rat videos used in this experiment but presents an interesting avenue of being able to fine tune segmentation processes to the morphology of different eyes.

VI. CONCLUSION

As shown in this analysis, retinal vessel pulsation in response to IOP exceeding ICP can be detected automatically with an accuracy of 77%. This may provide a new way to achieve rapid, non-invasive ICP monitoring. With further development, automated pulsatility detection of optic nerve veins may be applied to aid in the assessment of trauma patients.

ACKNOWLEDGMENT

This work was supported by the Hirshom Foundation grant and a University of Melbourne seed grant.

REFERENCES

- [1] J. D. Pickard and M. Czosnyka, "Management of raised intracranial pressure," *J. Neurol. Neurosurg. Psychiatry*, vol. 56, no. 8, pp. 845–858, Aug. 1993, doi: 10.1136/jnnp.56.8.845.
- [2] P. H. Raboel, J. Bartek, M. Andresen, B. M. Bellander, and B. Romner, "Intracranial Pressure Monitoring: Invasive versus Non-Invasive Methods—A Review," *Crit. Care Res. Pract.*, vol. 2012, p. 950393, 2012, doi: 10.1155/2012/950393.
- [3] M. Smith, "Monitoring Intracranial Pressure in Traumatic Brain Injury," *Anesth. Analg.*, vol. 106, no. 1, pp. 240–248, Jan. 2008, doi: 10.1213/01.ane.0000297296.52006.8e.
- [4] L. Rangel-Castillo, S. Gopinath, and C. S. Robertson, "Management of Intracranial Hypertension," *Neurologic Clinics*, vol. 26, no. 2, W.B. Saunders, pp. 521–541, 2008, doi: 10.1016/j.ncl.2008.02.003.
- [5] M. Baurman, "Über die Entstehung und klinische Bedeutung des Netzhautvenenpulses," *DtschOphthalmol Ges*, vol. 45, pp. 53–59, 1925.
- [6] E. N. Rios-Montenegro, D. R. Anderson, and N. J. David, "Intracranial Pressure and Ocular Hemodynamics."
- [7] H. W. Querfurth, P. Lieberman, S. Arms, S. Mundell, M. Bennett, and C. van Horne, "Ophthalmodynamometry for ICP prediction and pilot test on Mt. Everest," *BMC Neurol.*, vol. 10, p. 106, 2010, doi: 10.1186/1471-2377-10-106.
- [8] C. W. Mann, "Measurement of heart rate in white rat. I. The effects of anesthetization," *J. Comp. Psychol.*, vol. 34, no. 2, pp. 173–178, Oct. 1942, doi: 10.1037/h0063602.
- [9] S. Lu, "Accurate and Efficient Optic Disc Detection and Segmentation by a Circular Transformation," vol. 30, no. 12, pp. 2126–2133, 2011, doi: 10.1109/tmi.2011.2164261.
- [10] J. Odstreilik *et al.*, "Retinal vessel segmentation by improved matched filtering: evaluation on a new high-resolution fundus image database," *IET Image Process.*, vol. 7, no. 4, pp. 373–383, 2013, doi: 10.1049/iet-ipr.2012.0455.
- [11] H. Niemann *et al.*, "Towards automated diagnostic evaluation of retina images," *Pattern Recognit. Image Anal.*, vol. 16, no. 4, pp. 671–676, 2006, doi: 10.1134/s1054661806040146.